Konya Mühendislik Bilimleri Dergisi, c. 10, s. 2, 366-375, 2022
Konya Journal of Engineering Sciences, v. 10, n. 2, 366-375, 2022
ISSN: 2667-8055 (Electronic)
DOI: 10.36306/konjes.1003916

DETERMINATION OF OPTIMAL CONJUGATE GRADIENT METHOD FOR GEOMETRY FITTING

[1,2]Kadir KIRAN

[1] *Department of Airframe and Powerplant Maintenance, School of Civil Aviation, Suleyman Demirel University, Isparta, TURKEY*
[2] *Design and Manufacturing Laboratory, Innovative Technologies Application and Research Center (YETEM), Suleyman Demirel University, Isparta, TURKEY*
[1,2] kadirkiran@sdu.edu.tr

(Geliş/Received: 02.10.2021; Kabul/Accepted in Revised Form: 07.04.2022)

ABSTRACT: In this study, it is aimed to determine the optimal conjugate gradient (CG) method for the geometry fitting of 2D measured profiles. To this end, the three well-known CG methods such as the Fletcher-Reeves, Polak-Ribiere and Hestenes-Stiefel were employed. For testing those methods performances, the five primitive geometries accommodating circle, square, triangle, ellipse and rectangle were first built with a 3D printer, and then they were scanned with a coordinate measuring machine (CMM) to achieve their 2D profiles. The nonlinear least squares procedure was implemented to minimize the error between those measured data and modeled ones. An iterative line search was utilized for this task. The search direction was calculated using the above-mentioned CG methods. During the geometry fitting process, the number of function evaluations at each iteration were computed and the total number of function evaluations were set to be a performance measure of the CG method in question when it converged. By using these performance measures, the performance and data profiles were created to efficiently determine the optimal CG method. Based on performance profiles, it can be stated that the Fletcher-Reeves and Polak-Ribiere methods are the fastest ones on three test geometries out of five. In addition to that, all the CG methods were able to complete the geometry fitting of 80% of test geometries. On the other hand, by examining the data profiles, it was determined that the Polak-Ribiere and Hestenes-Stiefel methods achieve their maximum capabilities of the completing geometry fitting (i.e., 80%) with much lower number of function evaluations than the Fletcher-Reeves method. Besides, in most geometries, the Polak-Ribiere method outperformed the others, thereby it was determined to be the optimal one for the geometry fitting. As a conclusion, the reported results in this work might help the end-users who study on the CMM data processing to conduct an efficient geometry fitting.

Key Words: *Conjugate gradient, Geometry fitting, Optimization*

Geometri Uydurma için En İyi Eşlenik Gradyan Yönteminin Tespit Edilmesi

ÖZ: Bu çalışmada, ölçülen 2B profillere geometri uydurulması için en iyi eşlenik gradyan (EG) yönteminin tespit edilmesi hedeflenmektedir. Bu amaçla, iyi bilinen üç eşlenik gradyan yöntemleri, Fletcher-Reeves, Polak-Ribiere and Hestenes-Stiefel kullanıldı. Adı geçen yöntemlerin performansları test etmek için daire, kare, üçgen, elips ve dikdörtgen geometrilerini içeren test parçaları ilk olarak 3B yazıcı ile imal edildi ve daha sonra bu geometrilerin 2B profillerini elde etmek amacıyla adı geçen geometriler koordinat ölçme makinesi ile tarandı. Ölçülerek ve modellenerek elde edilen veriler arasındaki hatayı en aza indirmek için doğrusal olmayan en küçük kareler prosedürü uygulandı. Bu uygulama için bir iterativ doğru boyunca arama gerçekleştirildi. Arama yönü ise yukarıda adı geçen yöntemler kullanılarak hesaplandı. Geometri uydurma sürecinde her bir iterasyonda yapılan fonksiyon değerlendirme sayısı hesap edildi ve ilgili

eşlenik gradyan yöntemi yakınsadığında ortaya çıkan toplam fonksiyon değerlendirme sayısı yöntemin performans ölçütü olarak belirlendi. Verimli bir şekilde en iyi eşlenik gradyan yöntemini tespit edebilmek için bu performans ölçütleri kullanılarak performans ve veri profilleri oluşturuldu. Performans profillerine dayanarak, Fletcher-Reeves ve Polak-Ribiere yöntemlerinin beş geometriden üçünde en hızlı olduğu ifade edilebilir. Buna ek olarak, tüm EG yöntemleri test geometrilerinin %80'inin geometri uydurmasını tamamlayabilmiştir. Öte yandan, veri profilleri incelenerek, Polak-Ribiere ve Hestenes-Stiefel yöntemlerinin Fletcher-Reeves yöntemine göre çok daha az sayıda fonksiyon değerlendirmesi ile maksimum geometri uydurma kabiliyetlerine (%80) ulaştıkları tespit edilmiştir. Ayrıca birçok geometride Polak-Ribiere yöntemi diğerlerinden daha iyi olduğundan bu yöntem geometri uydurma için en iyi yöntem olarak belirlendi. Sonuç olarak, çalışmada rapor edilen sonuçlar koordinat ölçme makinesi verilerinin işlenmesi ile ilgilenen son kullanıcılara verimli bir geometri uydurma gerçekleştirmelerinde yardımcı olabilir.

Anahtar Kelimeler: *Eşlenik gradyan, Geometri uydurma, En iyileme*

1. INTRODUCTION

The application of the CG methods can be found in many fields such as engineering, computer science, etc. due to their efficiency in nonlinear optimization. Li et al. (2020), for instance, proposed a CG method along with pseudospectral collocation scheme. They applied it to find optimal rocket landing guidance. The authors reported that the proposed method stands out with high convergence speed and computational efficiency. In the work completed by Chattopadhyay and Chattopadhyay (2018), a neurocomputing model was developed using CG method-based backpropagation in artificial neural network for predicting average rainfall. An application of CG methods in finite element method was presented by Schwarz (1979). Helmig et al. (2020) investigated effect of number of temperature measurements on boundary conditions obtained using CG method. To this end, they used two test cases including orthogonal cutting process and a heat spreader cooling concept for power electronics and they stated that it is possible to reconstruction of the boundary using lower temperature measurements than the actual unknown boundary segments with a certain threshold number of sensors. Another study on inverse heat conduction problem was completed by Xiong et al. (2020) using a sequential CG method. They estimated the surface heat flux and it was reported that the proposed method provides more accurate results and less computation time. On the other hand, from the structural engineering point of view, Wang et al. (2013) revealed a new CG method for multi-source dynamic load identification from the noisy response measurements. The application results proved that the suggested method is more efficient than the Landweber iteration method. Moreover, for the image restoration problem, some modified Hestenes-Stiefel conjugate gradient algorithms were presented by Hu et al. (2020). Other CG algorithms (Cao and Wu, 2020; Joo et al., 1997), for this purpose, were also brought in the literature. In addition to them, some improved CG methods such as those of (Mtagulwa and Kaelo, 2019; Jiang and Jian, 2019; Wang et al., 2018; Fatemi, 2016) were presented for general optimization problems.

As can be seen from the above summarized studies, the CG methods have been frequently finding an area to be applied. However, no study was found on the geometry fitting and the CMM data processing by using CG methods. Thus, there is no data about their performance in this topic. To a little contribute this gap, the current work concentrates on defining the optimal CG methods from the well-known methods (i.e., Fletcher-Reeves, Polak-Ribiere and Hestenes-Stiefel) for the geometry fitting of measured 2D profiles. The paper is structured as follows: Section 2. covers the primitive geometries, their mathematical models, and the geometry fitting procedure. A brief description on the mathematical background of CG method is given in Section 3. In Section 4, the obtained results are presented with discussion. Finally, Section 5 summarizes and concludes the paper.

Nomenclature			
x, y:	coordinates of each point on the geometry	r_c:	radius of circle
x_u, y_u:	coordinates of each point on the geometry without rotation	r:	radius of triangle
x_c, y_c:	center coordinates of the geometry	θ:	rotation angle
u:	parameter ranging between 0 and 2π radians	a:	radius of ellipse along x axis
w:	width	b:	radius of ellipse along y axis
h:	height	n_s:	Number of edges (i.e., $n_s = 3$ for triangle)

2. PRIMITIVE GEOMETRIES AND THEIR FITTING PROCEDURE

For determination of the optimal CG method, the five primitive geometries are used. Those geometries are circle, square, rectangle, triangle, and ellipse. Their parametric mathematical models (Desmos, 2021) are given below.

Circle:

$$\begin{aligned} x &= r_c \cos(u) + x_c \\ y &= r_c \sin(u) + y_c \end{aligned} \tag{1}$$

Square and rectangle:

$$\begin{aligned} x_u &= \frac{w}{2}(|\cos(u)|\cos(u) + |\sin(u)|\sin(u)) \\ y_u &= \frac{h}{2}(|\cos(u)|\cos(u) - |\sin(u)|\sin(u)) \\ x &= x_u \cos(\theta) - y_u \sin(\theta) + x_c \\ y &= x_u \sin(\theta) + y_u \cos(\theta) + y_c \end{aligned} \tag{2}$$

Triangle:

$$\begin{aligned} r &= \frac{h}{cos\left(\frac{2}{n_s} arcsin\left(sin\left(\frac{n_s}{2}u\right)\right)\right)} \\ x_u &= r\, cos(u) \\ y_u &= r\, sin(u) \\ x &= x_u\, cos(\theta) - y_u\, sin(\theta) + x_c \\ y &= x_u\, sin(\theta) + y_u\, cos(\theta) + y_c \end{aligned} \tag{3}$$

Ellipse:

$$\begin{aligned} x_u &= a\cos(u) \\ y_u &= b\sin(u) \\ x &= x_u \cos(\theta) - y_u \sin(\theta) + x_c \\ y &= x_u \sin(\theta) + y_u \cos(\theta) + y_c \end{aligned} \tag{4}$$

All those coordinate calculations given above are theoretical. To obtain actual coordinates of those geometries, first a workpiece containing those geometries were built using a 3D printer with a PLA material. They were later scanned via the CMM that provides their 2D profiles. With these theoretical and measured data, the nonlinear least squares fitting procedure is employed. To do so, first we describe the sum of the squared errors, $\epsilon^2(p)$, between theoretical and measured data as follows (Jia, 2017):

$$\epsilon^2(p) = \sum_{j=1}^{n}\left[x_j - x_j^{model}(p)\right]^2 + \sum_{j=1}^{n}\left[y_j - y_j^{model}(p)\right]^2 \quad (5)$$

where p is the parameter vector accommodating all the variables in the geometry being used, x_j, y_j, $x_j^{model}(p)$ and $y_j^{model}(p)$ denote x and y-coordinates of the geometry obtained from the measurement and the mathematical model, respectively. As well-known, the nonlinear least squares procedure aims to minimize this parameter dependent error. For that purpose, in this study, an iterative line search procedure along with three well-known CG methods is implemented. The details about the minimization process are covered in the next section.

3. CONJUGATE GRADIENT METHODS

The conjugate gradient methods are frequently used in nonlinear optimization problems. To minimize the sum of squared errors between the data obtained via the measurements and the mathematical model, in this study, an iterative line search procedure is implemented. In the line search, the search direction, s_{j+1}, (see Equation 6.) is computed using three well-known CG methods (i.e., Fletcher-Reeves (Fletcher and Reeves, 1964), Polak-Ribiere (Polak and Ribiere, 1969) and Hestenes-Stiefel (Hestenes and Stiefel, 1952)).

$$s_{j+1} = -G\left(p_{j+1}\right) + \beta_{j+1}s_j \quad (6)$$

In this equation, $G = -J^T D$ is the objective function gradient, J is the Jacobian matrix of the objective function, $D = \begin{bmatrix} D_x \\ D_y \end{bmatrix}$ is the difference matrix, $D_x = x_j - x_j^{model}(p)$ and $D_y = y_j - y_j^{model}(p)$. β_{j+1} is the CG coefficient and it is computed using the above-mentioned methods. Their mathematical descriptions are given below.

Fletcher-Reeves:

$$\beta_{j+1} = \frac{G(p_{j+1})^T G(p_{j+1})}{G(p_j)^T G(p_j)} \quad (7)$$

Polak-Ribiere:

$$\beta_{j+1} = \frac{G(p_{j+1})^T\left(G(p_{j+1}) - G(p_j)\right)}{\|G(p_j)\|^2} \quad (8)$$

Hestenes-Stiefel:

$$\beta_{j+1} = \frac{G(p_{j+1})^T\left(G(p_{j+1}) - G(p_j)\right)}{s_j^T\left(G(p_{j+1}) - G(p_j)\right)} \quad (9)$$

In Equations 7 to 9, the initial search direction is $s_0 = -G(p_0)$ (i.e., opposite of the gradient of the objective function). By using all those, the iterative line search to find the next parameters is describes as follows (Nocedal and Wright, 2006):

$$p_{j+1} = p_j + \alpha_j s_j^T \quad (10)$$

where $\alpha_j > 0$ is the step length that controls the amount of the movement along the CG direction. It can be computed using various line search conditions. However, in this study, a numerical algorithm is

implemented to compute the step length. Equation 10 proceeds until the convergence condition is satisfied. This condition is:

$$\text{maximum}|J^T D| \leq \partial \qquad (11)$$

where $\partial = 10^{-4}$ is the convergence tolerance.

4. RESULTS AND DISCUSSION

To determine the optimal CG method for geometry fitting, totally fifteen geometry fittings have been completed using the five test geometries and three CG methods. For keeping track the geometry fitting process, the geometry fitting parameters, sum of the squared errors, norm of the gradient of the objective function and step length have been recorded at each iteration. Those results are presented in Figure 1. Note that all those results, as example, belong the ellipse fitting process with the Polak-Ribiere method. The same procedure has been also completed for all the test geometries and the CG methods. In addition, the number of function evaluations (Nfe), as the performance measure of the CG method, are computed for each iteration. The above-mentioned fitting outcomes are also plotted in accordance with number of function evaluations, as shown in Figure 2.

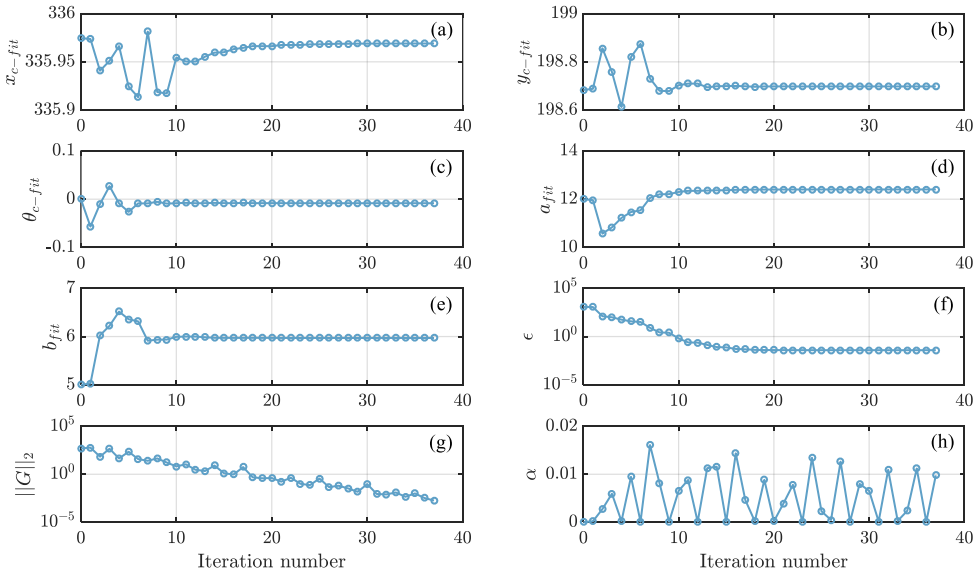

Figure 1. Fitting progress of the ellipse: Results versus iteration, (a) Ellipse center x-coordinate (mm) (b) Ellipse center y-coordinate (mm) (c) Ellipse rotation angle (degree) (d) Ellipse radius along x-direction (mm) (e) Ellipse radius along y-direction (mm) (f) Sum of squared errors (g) Norm of the gradient of objective function (h) Step length

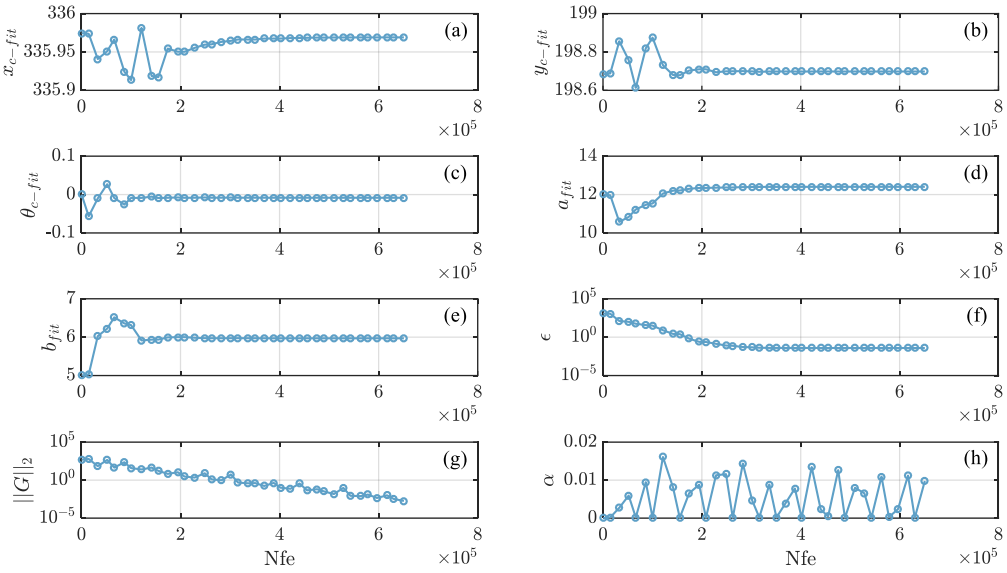

Figure 2. Fitting progress of the ellipse: Results versus number of function evaluations, (a) Ellipse center x-coordinate (mm) (b) Ellipse center y-coordinate (mm) (c) Ellipse rotation angle (degree) (d) Ellipse radius along x-direction (mm) (e) Ellipse radius along y-direction (mm) (f) Sum of squared errors (g) Norm of the gradient of objective function (h) Step length

As can be seen from these figures, the iterative line search starts with initial parameter values supplied by the user and it successfully converges the required tolerance after a little bit fluctuation. It might be stated that the convergence is linear based on the Figure 2(g). Also notice that the sum of squared error and norm of the gradient of the objective function continuously decrease. This shows that the proposed fitting process works very well. On the other hand, the number of function evaluations at each iteration quite different due to step length computation. Figure 2(h) shows that the different step length is necessary for a significant progress, which means that the amount of work, the number of function evaluations, will vary during the process. As a result of converged ellipse parameters at 37. iteration (i.e., $x_c = 335.9690$ mm, $y_c = 198.6981$ mm, $\theta = -0.0084^o$, $a = 12.4034$ mm, $b = 5.97$ mm), a comparison of actual, fit, and measured ellipses is indicated in Figure 3. One can notice that the fitted ellipse successfully represents the measured data.

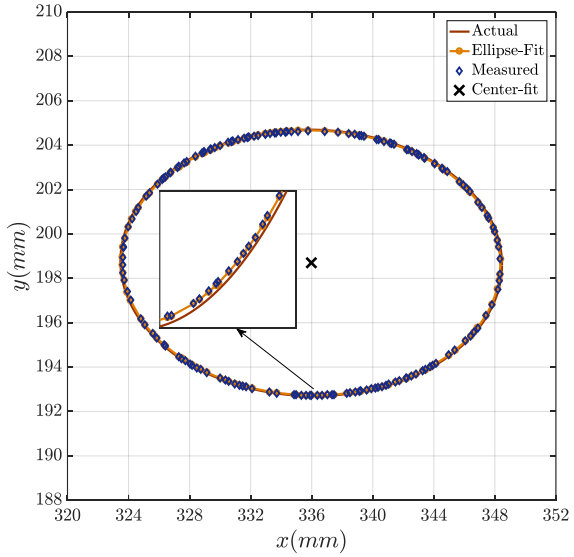

Figure 3. Ellipse fitting

As mentioned before, the same outcome recording procedure (i.e., Figures 1 and 2) and the fit quality check (i.e., Figure 3) have been completed for all the test geometries and the CG methods. At the end of convergence, the total number of function evaluations are set as the performance measure of the CG methods for each geometry. All those results are provided in Figure 4. The geometry numbers 1, 2, 3, 4 and 5, in this figure, correspond to the circle, the square, the triangle, the ellipse and the rectangle, respectively. Moreover, the ∞ denotes that the corresponding CG method fails to converge. For more clarity, the Fletcher-Reeves on the square, Polak-Ribiere and Hestenes-Stiefel on the rectangle are not successful to complete the fitting process.

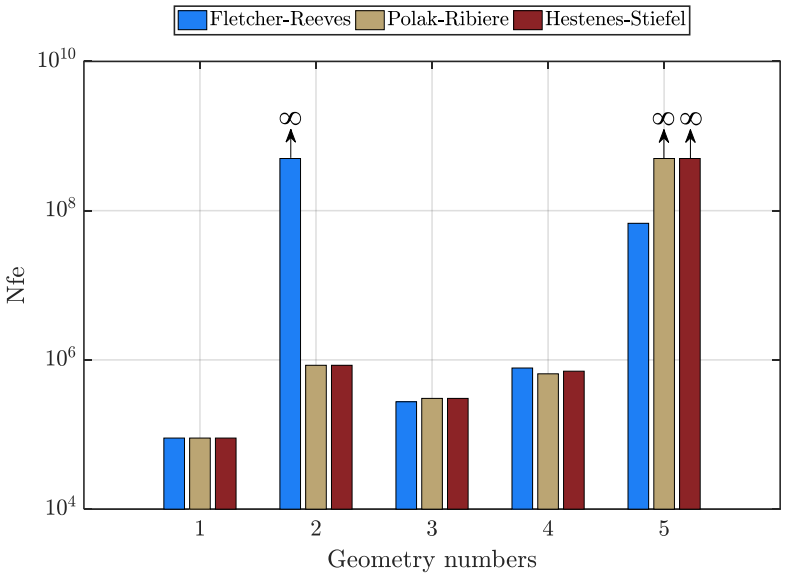

Figure 4. Total number of function evaluations for all CG methods

One can also notice from Figure 4. that the Polak-Ribiere and Hestenes-Stiefel methods exhibit similar performances for all the geometries while the Fletcher-Reeves differs from them on the geometries 2 and 5. It can be seen that, for rectangle fit, the Fletcher-Reeves is the only one being successful. Although those interpretations, it is difficult to define the optimal CG method for geometry fitting. Therefore, we generate performance (Dolan and More, 2002) and data profiles (More and Wild, 2009) using the total number of function evaluations. The performance profiles of the CG methods are illustrated in Figure 5. These profiles simply show success rate of the CG methods within the factor υ of the fastest CG method which can be identified from probability values $P(\upsilon)$ at $\upsilon = 1$. Such that, the fastest CG method might be defined either the Fletcher-Reeves and the Polak-Ribiere. Both has $P(1) = 60\%$, which means that they are the fastest one on three test geometries out of five, whereas the Hestenes-Stiefel has the probability $P(1) = 40\%$. As we keep increasing factor υ, all the methods capabilities to complete geometry fitting rise. For instance, at the factor $\upsilon = 1.109$ of fastest one, the Polak-Ribiere and the Hestenes-Stiefel methods performances rise to 80% (i.e., $P(1.109\ ) = 80\%$). At this factor, the Fletcher-Reeves method performance remains same. It can be also mentioned that the Polak-Ribiere and the Hestenes-Stiefel methods reach up their maximum performance at $\upsilon = 1.109$. From this value on, even if we increase the υ, their success probability will not change. However, the same is not valid for the Fletcher-Reeves. It is necessary to increase the factor υ from 1.109 to 1.196. At this value, the Fletcher-Reeves reaches its maximum probability (i.e., $P(1.196\ ) = 80\%$).

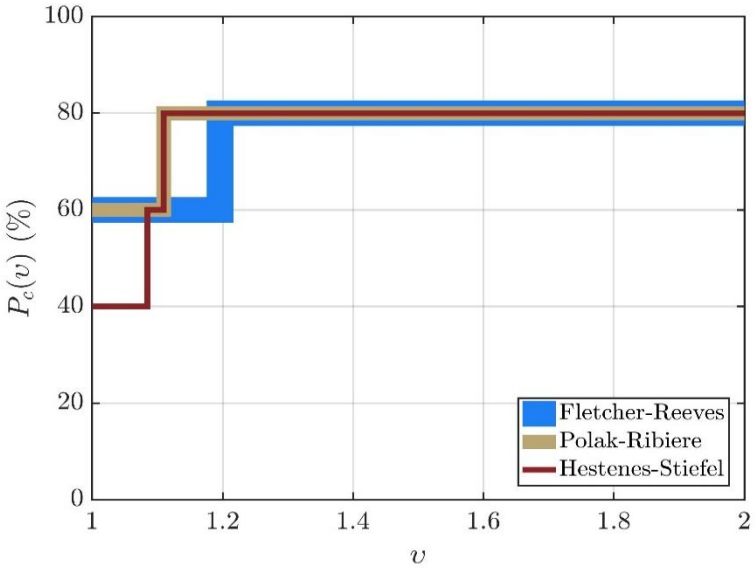

Figure 5. Performance profiles of CG methods

In other respect, we can also evaluate the performances of the CG methods from a computational budget perspective. For this task, we use data profiles, as shown Figure 6. Those profiles basically provide the number of geometries, which can be successfully fitted by the CG methods, within given computational budget (i.e., total number of function evaluations in this study). As an example, we are given a computational budget of 5×10^5 (i.e., $\psi = 5 \times 10^5$) total number of function evaluations to complete at least two geometry fittings (i.e., $D(\psi = 5 \times 10^5) \geq 40\%$). In these terms, we could choose one of the CG methods because they all have same probability $D(\psi = 5 \times 10^5) = 40\%$. Let's give another example; the computational budget is $\psi = 6.51 \times 10^5$ and we need to fit at least three geometries ($D(\psi = 6.51 \times 10^5) \geq 60\%$). For these conditions, the only choice is the Polak-Ribiere method because its probability at $\psi = 6.51 \times 10^5$ is 60% while the others have probability of 40% (see Figure 6). As can be seen from the figure that the Polak-Ribiere and Hestenes-Stiefel methods reach maximum number of geometry fitting (i.e., 4 geometries out of 5) at $\psi = 8.472 \times 10^5$. However, the Fletcher-Reeves requires much greater number of function evaluations to reach the $D(\psi) = 80\%$.

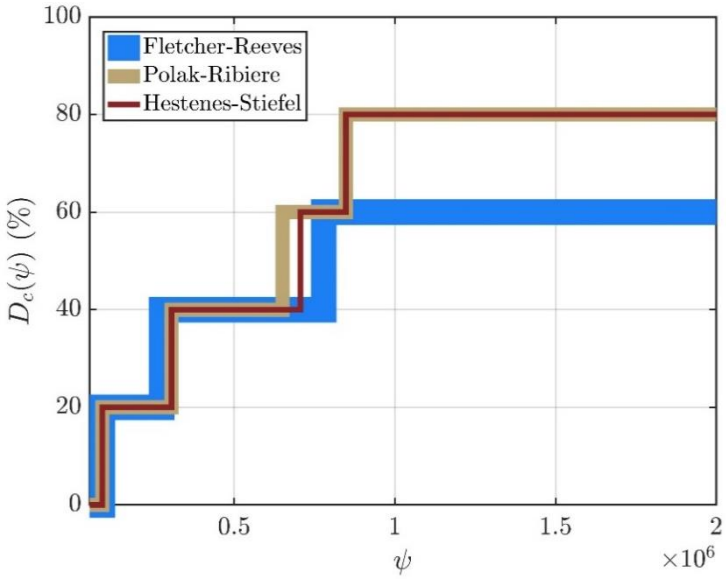

Figure 6. Data profiles of CG methods

Based on the results reported so far, it is determined that the Polak-Ribiere is the optimal CG method for geometry fitting in this study because it is both one of the fastest methods and requires lower number of function evaluations to reach the maximum probability compared to others. This efficiency of the Polak-Ribiere method comes from its self-restarting property. More specifically, if the method provides a bad search direction and a small progress (i.e., $p_{j+1} \approx p_j$ which in turn $G(p_{j+1}) \approx G(p_j)$), the β_{j+1} will be approximately zero (see Equation 8). In this case, the method reduces to steepest descent method, which means that it restarts itself to get rid of bad search direction and small progress. The same property is also valid for the Hestenes-Stiefel method. However, the Fletcher-Reeves method is not able to perform a self-restarting and it requires additional restart conditions in this case. For further mathematical details on this property, the reader is referred to Nocedal and Wright (2006).

5. CONCLUSIONS

This paper has focused on determining the optimal CG method for geometry fitting. For this task, the three well-known CG methods (i.e., Fletcher-Reeves, Polak-Ribiere and Hestenes-Stiefel) were employed. To test their performances in the geometry fitting, the five primitive geometries such as circle, square, triangle, ellipse and rectangle were selected and their 2D profiles were acquired via the CMM. Based on the nonlinear least squares fitting process, the sum of the squared error between the measured and modeled data was minimized using the iterative line search along with the conjugate directions obtained from the above-mentioned CG methods. During the fitting process, the number of function evaluations required to progress in the line search were kept track for each iteration, and the total number of function evaluations, when the CG method being used converges, were set as a performance measure. Using those data, the performance and data profiles were created to be efficiently determine the optimal method. The results have shown that the Fletcher-Reeves and the Polak-Ribiere are the fastest ones based on the performance profiles. However, for an optimal choice, it has been determined that the Polak-Ribiere is a great candidate. From a practical application view, those results may be pioneer for the end-users who deal with geometry fitting of the CMM data.

6. ACKNOWLEDGEMENT

The author thanks Design and Manufacturing Laboratory, Innovative Technologies Application and Research Center (YETEM), Suleyman Demirel University where provides the scanning of the geometries used in this study with the CMM.

REFERENCES

Cao, J., Wu, J., 2020, "A conjugate gradient algorithm and its applications in image restoration", *Applied Numerical Mathematics*, 152, 243-252.

Chattopadhyay, S., Chattopadhyay, G., 2018, "Conjugate gradient descent learned ANN for Indian summer monsoon rainfall and efficiency assessment through Shannon-Fano coding", *Journal of Atmospheric and Solar-Terrestrial Physics*, 179, 202-205.

Desmos, https://www.desmos.com, Access date:16.05.2021.

Dolan, E.D., More, J.J., 2002, "Benchmarking optimization software with performance profiles", *Mathematical programming*, 91, 201-213.

Fatemi, M., 2016, "A new efficient conjugate gradient method for unconstrained optimization", *Journal of Computational and Applied Mathematics*, 300, 207-216.

Fletcher, R., Reeves, C.M., 1964, "Function minimization by conjugate gradients", *The Computer Journal*, 7(2), 149-154.

Helmig, T., Al-Sibai, F., Kneer, R., 2020, "Estimating sensor number and spacing for inverse calculation of thermal boundary conditions using the conjugate gradient method", *International Journal of Heat and Mass Transfer*, 153, 119638.

Hestenes, M.R., Stiefel, E. 1952, "Methods of conjugate gradients for solving linear systems", *Journal of Research of the National Bureau of Standards*, 49(6), 409-436.

Hu, W., Wu, J., Yuan, G., 2020, "Some modified Hestenes-Stiefel conjugate gradient algorithms with application in image restoration", *Applied Numerical Mathematics*, 158, 360–376.

Jia, P., 2017, *Fitting a parametric model to a cloud of points via optimization methods*, Ph.D. thesis, Syracuse University, New York.

Jiang, X., Jian, J., 2019, "Improved Fletcher–Reeves and Dai–Yuan conjugate gradient methods with the strong Wolfe line search", *Journal of Computational and Applied Mathematics*, 348, 525-534.

Joo, K. S., Bose, T., Xu, G. F., 1997, "Image restoration using a conjugate gradient-based adaptive filtering algorithm", *Circuits systems signal processing*, 16(2), 197-206.

Li, Y., Chen, W., Zhou, H., Yang, L., 2020, "Conjugate gradient method with pseudospectral collocation scheme for optimal rocket landing guidance", *Aerospace Science and Technology*, 104, 105999.

More, J. J., Wild, S. M., 2009, "Benchmarking derivative-free optimization algorithms", *SIAM Journal on Optimization*, 20, 172-191.

Mtagulwa, P., Kaelo, P., 2019, "An efficient modified PRP-FR hybrid conjugate gradient method for solving unconstrained optimization problems", *Applied Numerical Mathematics*, 145, 111–120.

Nocedal, J., Wright, S.J., 2006, *Numerical optimization*, 2nd ed., Springer Science & Business Media, New York.

Polak, E., Ribiere, G., 1969, "Note sur la convergence de methodes de directions conjuguees. Revue francaise d'informatique et de recherche operationnelle", *Revue francaise d'informatique et de recherche operationnelle*, 3(R1), 35-43.

Schwarz, H. R., 1979, "The Method of Conjugate Gradients in Finite Element Applications", *Journal of Applied Mathematics and Physics*, 30, 342-354.

Wang, L., Han, X., Xie, Y., 2013, "A new conjugate gradient method for solving multi-source dynamic load identification problem", *Int J Mech Mater Des*, 9, 191-197.

Wang, J., Zhang, B., Sun, Z., Hao, W. and Sun, Q., 2018, "A novel conjugate gradient method with generalized Armijo search for efficient training of feedforward neural networks", *Journal of Neurocomputing*, 275, 308-316.

Xiong, P., Deng, J., Lu, T., Lu, Q., Liu, Y., Zhang, Y., 2020, "A sequential conjugate gradient method to estimate heat flux for nonlinear inverse heat conduction problem", *Annals of Nuclear Energy*, 149, 107798.